

A Dynamic Model of Reaction Pathway Effects on Parahydrogen-Induced Nuclear Spin Polarization

Gerd Buntkowsky,^{1a} Joachim Bargon,^{1b} and Hans-Heinrich Limbach*,^{1a}

Contribution from the Institut für Organische Chemie der Freien Universität Berlin, Takustrasse 3, D-14195 Berlin, and Institut für Physikalische Chemie der Universität Bonn, Wegelerstrasse 12, D-53115 Bonn, Germany

Received December 13, 1995[®]

Abstract: A dynamic model for the calculation of parahydrogen (p-H₂) induced nuclear polarization (PHIP) of hydrogenation products is described which is based on the density matrix formalism. This formalism was proposed previously by Binsch for the calculation of NMR spectra broadened by chemical exchange between different sites. Using numerical simulations typical for actual experiments, it is shown that the PHIP patterns may depend not only on the type of experiment performed—e.g., ALTADENA (adiabatic longitudinal transport after dissociation engenders net alignment) in the absence and PASADENA (parahydrogen and synthesis allow dramatically enhanced nuclear alignment) in the presence of a magnetic field—but also on the pathways of the hydrogenation reaction, in which generally transition metal catalysts are involved. Of particular importance are the properties of possible reaction intermediates where the reactants are complexed alone or together to the catalyst. Indirect information from the PHIP pattern of the hydrogenation products on the intermediate can be obtained, in particular its chemical shifts, exchange and magnetic couplings, and the incoherent dihydrogen self-exchange. In addition, the regioselectivity of the hydrogenation step is a factor influencing the PHIP patterns. The model and the results obtained here provide, therefore, a theoretical link between various phenomena concerning the hydrogen mobility in transition metal catalysts, and PHIP is shown to be a valuable tool for obtaining information on the reaction intermediates.

Introduction

The problem of the mobility of hydrogen in transition metal complexes is a long-standing challenging experimental and theoretical problem.^{2,3} Wilkinson found the first catalysts which are able to take up and easily activate molecular dihydrogen during the hydrogenation of double bonds (Figure 1).² Interesting insights into this phenomenon have been obtained in recent years by the proposition of Bowers and Weitekamp⁴ to use parahydrogen (p-H₂) as a diagnostic tool in hydrogenation reactions. p-H₂ exhibits a pure nuclear singlet state associated via the Pauli exclusion principle with the lowest rotational state, and is stable even in liquid solutions.⁵ The transformation of this molecular rotational order into nuclear spin order during the hydrogenation reaction leads to typical polarization patterns in the NMR spectra of the hydrogenation products. These types of experiments have been referred to under the acronym PASADENA (parahydrogen and synthesis allow dramatically enhanced nuclear alignment),⁴ or more generally PHIP (parahydrogen-induced polarization).^{6,7} When the reaction is carried out in the absence of a magnetic field and the sample is then

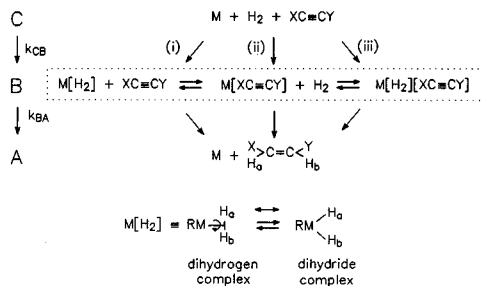


Figure 1. Possible pathways of the catalyzed hydrogenation reaction of an unsaturated organic substrate involving various transition metal dihydrogen and/or dihydride intermediates. The initial free dihydrogen is labeled as site C, the intermediates containing the dihydrogen pair are labeled as B, and the product containing the dihydrogen pair is labeled as A.

adiabatically introduced into the NMR spectrometer, the effects are different and named ALTADENA (adiabatic longitudinal transport after dissociation engenders net alignment).⁴ The PHIP theory of Bowers and Weitekamp⁴ treats the case such that the symmetry of p-H₂ is broken either suddenly in the PASADENA or slowly in the ALTADENA experiment during the incorporation of dihydrogen into the reaction product, wherein the two protons form a first-order AX spin system.

A consequence of this simple treatment is that the PHIP patterns of the product are not supposed to reveal any information concerning the reaction pathway, especially on potential intermediates of the reaction, where dihydrogen is bound to the transition metal catalyst, either alone or together with the substrate, as indicated in Figure 1. Whereas transition metal

[®] Abstract published in *Advance ACS Abstracts*, August 15, 1996.

(1) (a) Freie Universität Berlin. (b) Universität Bonn.

(2) Osborn, J. A.; Jardine, F. H.; Young, J. F.; Wilkinson, G. J. *J. Chem. Soc. A* **1966**, 1711.

(3) Brown, J. M.; Evans, P.; Lucy, A. R. *J. Chem. Soc., Perkin Trans 2* **1987**, 1591.

(4) (a) Bowers, C. R.; Weitekamp, D. P. *Phys. Rev. Lett.* **1986**, 57, 2645.

(b) Pravica, M. G.; Weitekamp, D. P. *Chem. Phys. Lett.* **1988**, 145, 255.

(c) Bowers, C. R.; Weitekamp, D. P. *J. Am. Chem. Soc.* **1987**, 109, 554.

(d) Bowers, C. R.; Jones, D. H.; Kurur, N. D.; Labinger, J. A.; Pravica, M. G.; Weitekamp, D. P. *Adv. Magn. Reson.* **1990**, 15, 269.

(5) (a) Silvera, I. F. *Rev. Mod. Phys.* **1980**, 52, 393. (b) van Kranendonk, J. *Solid Hydrogen*; Plenum: New York, 1983. (c) Abragam, A. *The Principles of Nuclear Magnetism*; Clarendon Press: Oxford, 1961.

(6) (a) Eisenschmidt, T. C.; Kirss, R. U.; Deutsch, P. P.; Hommeltoft, S. I.; Eisenberg, R.; Bargon, J. *J. Am. Chem. Soc.* **1987**, 109, 8089. (b) Kirss, R. U.; Eisenschmidt, T.; Eisenberg, R. *J. Am. Chem. Soc.*, **1988**, 110, 8564. (c) Eisenberg, R. *Acc. Chem. Res.* **1991**, 24, 110.

(7) (a) Bargon, J.; Kandels, J.; Woelk, K. *Z. Phys. Chem.* **1993**, 180, 65.

(b) Kating, P.; Wandelt, A.; Selke, R.; Bargon, J. *J. Phys. Chem.* **1993**, 97, 13313.

(c) Bargon, J.; Kandels, J.; Kating, P. *J. Chem. Phys.* **1993**, 98, 6150.

(d) Bargon, J.; Kandels, J.; Kating, P.; Thomas, A.; Woelk, K. *Tetrahedron Lett.* **1990**, 31, 5721.

(e) Bargon, J.; Kandels, J.; Woelk, K. *Angew. Chem.* **1990**, 102, 70; *Angew. Chem., Int. Ed. Engl.* **1990**, 29, 58.

hydride configurations involving M–H bonds have been known for a long time, the discovery of side-on dihydrogen configurations, i.e., M–[η -H₂] also included in Figure 1, has been made only recently by Kubas et al.^{8,9} The transition between the dihydrogen and the dihydride forms formulated in Figure 1 as a classical equilibrium may, however, be continuous.⁹ These transition metal complexes exhibit interesting properties. In particular, a number of complexes have been found whose NMR spectra exhibit unusually large NMR *J* couplings between nonequivalent metal bound hydrogen nuclei.^{10–15} The origin of this phenomenon has been identified by Zilm et al.¹³ and Weitekamp et al.^{4d,14} as arising from quantum exchange between hydrogen pairs, similar to the exchange interaction between electrons. Therefore, this phenomenon has been termed “exchange coupling”, in contrast to the usual magnetic spin–spin coupling. Exchange couplings can be interpreted as average tunnel splittings of a coherent dihydrogen exchange. They strongly increase with temperature until a point is reached where an incoherent stochastic or classical dihydrogen exchange is activated, rendering the hydrogen atoms pairwise equivalent. In this case, the NMR spectra are no longer affected by the exchange couplings. These phenomena are very puzzling up to date and still subject to a number of theoretical investigations.^{15–19}

In recent papers¹⁵ some of us have proposed a general model of coherent and incoherent dihydrogen exchange effects in the coordination sphere of transition metals. The model was formulated in terms of the line shape theory of Alexander and Binsch²⁰ using the quantum mechanical density matrix formalism. According to this model, the quantum exchange in

- (8) (a) Kubas, G. J.; Ryan, R. R.; Swanson, B. I.; Vergamini, P. J.; Wasserman, H. J. *J. Am. Chem. Soc.* **1984**, *106*, 451. (b) Kubas, G. J. *Acc. Chem. Res.* **1988**, *21*, 120. (c) Rattan, G.; Kubas, G. J.; Unkefer, C. J.; Van Der Sluys, L. S.; Kubat-Martin, K. A. *J. Am. Chem. Soc.* **1990**, *112*, 3855.
- (d) Eckert, J.; Kubas, G. J. *J. Phys. Chem.* **1993**, *97*, 2378.
- (9) Crabtree, R. H. *Acc. Chem. Res.* **1990**, *23*, 95.
- (10) (a) The NMR properties of Nb(C₅H₅)₂H₃ were discussed by Labinger, J. A. In *Comprehensive Organometallic Chemistry*; Wilkinson, G.; Stone, F. G. A.; Abel, E., Eds.; Pergamon Press: New York, 1983; Vol. 3, p 707, cited as unpublished results of F. N. Tebbe. (b) Arliguie, T.; Chaudret, B.; Devillers, J.; Poilblanc, R. C. *R. Acad. Sci., Ser. II* **1987**, *305*, 1523. (c) Antinolo, A.; Chaudret, B.; Commenges, G.; Fajardo, M.; Jalon, F.; Morris, R. H.; Otero, A.; Schweitzer, C. T. *J. Chem. Soc., Chem. Commun.* **1988**, 1210. (d) Arliguie, T.; Border, C.; Chaudret, B.; Devillers, J.; Poilblanc, R. *Organometallics* **1989**, *8*, 1308. (e) Arliguie, T.; Chaudret, B.; Jalon, F. A.; Otero, A.; Lopez, J. A.; Lahoz, F. J. *Organometallics* **1991**, *10*, 1888. (f) Chaudret, B.; Limbach, H. H.; Moise, C. C. *R. Acad. Sci., Ser. II*, **1992**, *315*, 533. (g) Sabo-Étienne, S.; Chaudret, B.; Abou el Makarim, H.; Barthelat, J. C.; Daudy, J. P.; Ulrich, S.; Limbach, H. H.; Moise, C. *J. Am. Chem. Soc.* **1995**, *117*, 11602.
- (11) Paciello, R. R.; Manriquez, J. M.; Bercaw, J. E. *Organometallics* **1990**, *9*, 260.
- (12) Heinekey, D. M.; Payne, N. G.; Schulte, G. K. *J. Am. Chem. Soc.* **1988**, *110*, 2303.
- (13) (a) Heinekey, D. M.; Millar, J. M.; Koetzle, T. F.; Payne, N. G.; Zilm, K. W. *J. Am. Chem. Soc.* **1990**, *112*, 909. (b) Zilm, K. W.; Heinekey, D. M.; Millar, J. M.; Payne, N. G.; Demou, P. J. *Am. Chem. Soc.* **1989**, *111*, 3088. (c) Zilm, K. W.; Heinekey, D. M.; Millar, J. M.; Payne, N. G.; Neshyba, S. P.; Duchamp, J. C.; Szczyrba, J. *J. Am. Chem. Soc.* **1990**, *112*, 920. (d) Zilm, K. W.; Millar, J. M. *Adv. Magn. Reson.* **1990**, *15*, 163. (e) Inati, S. J.; Zilm, K. W. *Phys. Rev. Lett.* **1992**, *68*, 3273. (f) Wisniewski, L. L.; Mediati, M.; Jensen, C. M.; Zilm, K. W. *J. Am. Chem. Soc.* **1993**, *115*, 7534.
- (14) Jones, D.; Labinger, J. A.; Weitekamp, J. *J. Am. Chem. Soc.* **1989**, *111*, 3087.
- (15) (a) Limbach, H. H.; Scherer, G.; Maurer, M.; Chaudret, B. *Angew. Chem.* **1992**, *104*, 1414; *Angew. Chem., Int. Ed. Engl.* **1990**, *31*, 1369. (b) Limbach, H. H.; Ulrich, S.; Buntkowsky, G.; Sabo-Étienne, S.; Chaudret, B.; Kubas, G. J.; Eckert, J. Submitted for publication.
- (16) Barthelat, J. C.; Chaudret, B.; Daudy, J. P.; De Loth, Ph.; Poilblanc, R. *J. Am. Chem. Soc.* **1991**, *113*, 9896.
- (17) Jarid, A.; Moreno, M.; Lledós, A.; Lluch, J. M.; Bertran, J. *J. Am. Chem. Soc.* **1993**, *115*, 5861.
- (18) (a) Hiller, E. M.; Harris, R. A. *J. Chem. Phys.* **1993**, *98*, 2077. (b) *Ibid.* **1993**, *99*, 7652. (c) *Ibid.* **1993**, *100*, 2522.
- (19) Szymanski, S. *J. Mol. Struct.* **1994**, *321*, 115.

transition metal hydrides is mainly caused by the thermal population of dihydrogen configurations, as either metastable species or specifically excited rovibrational states. It was shown that the coherent dihydrogen exchange does not transform into an incoherent exchange but that both processes are superimposed, each characterized by a different temperature dependence. This concept led to the idea to formulate the PHIP effects in terms of the quantum mechanical density matrix formalism, taking into account the whole reaction pathway of Figure 1, whereby the pathways of incoherent dihydrogen exchange and of the hydrogenation reaction partially coincide. This would allow all findings to be condensed, namely, the interconversion between dihydride and dihydrogen configurations, quantum exchange couplings, NMR line shapes, and inelastic neutron scattering line shapes^{8,15b} of transition metal hydrides as well as reaction path effects on PHIP patterns of hydrogenation products, into one compact model.

The goal of this work is to describe the reaction sequence outlined in Figure 1 using a density matrix approach and to analyze potential reaction path effects on the PHIP signal patterns of the hydrogenation products. Such reaction path effects depend on the properties of the intermediate states in which the nuclear spin symmetry of the dihydrogen is actually broken. Indeed, we have found such effects, and they are sensitive not only to the chemical shifts but also to the size of the coherent and the incoherent dihydrogen exchange in the intermediates. Therefore, the description presented here not only allows so far puzzling PHIP patterns to be interpreted but also leads to conclusions about the reaction pathways via analysis of these patterns.

This paper is organized as follows: in the theoretical section a short introduction into the PHIP phenomenon and a brief description of the quantum mechanical density matrix formalism is given, followed by a survey of the numerical methods used for solving the Liouville von Neumann equation. The results obtained using numerical calculations of PHIP effects expected for hydrogenation products that are formed either in a direct two-site hydrogenation reaction or in a three-site reaction involving an intermediate are then presented and discussed.

Theoretical Section

Introduction into PHIP. The origins of symmetry-induced nuclear polarization can be summarized as follows: as mentioned above and as illustrated in Figure 2, molecular dihydrogen is composed of two species, p-H₂, which is characterized by the product of a symmetric rotational wave function and an antisymmetric nuclear spin wave function ($|3\rangle = |S\rangle = 1/\sqrt{2}(|\alpha\beta\rangle - |\beta\alpha\rangle)$), and orthohydrogen (o-H₂), which is characterized by an antisymmetric rotational wave function and one of the symmetric nuclear spin wave functions ($|1\rangle = |T_+\rangle = |\alpha\alpha\rangle$, $|2\rangle = |T_0\rangle = 1/\sqrt{2}(|\alpha\beta\rangle + |\beta\alpha\rangle)$, $|4\rangle = |T_-\rangle = |\beta\beta\rangle$). In thermal equilibrium at room temperature each of the three ortho states and the single para state have practically all equal probability. By contrast at temperatures below that of liquid nitrogen, mainly the energetically lower para state is populated.⁵ Therefore, an enrichment of the para state and even the separation of the two species can be easily achieved at low temperatures as their interconversion is a rather slow process. Thus, p-H₂ enriched hydrogen can be stored and used subsequently for hydrogenation reactions.^{4–7}

As indicated in Figure 1, for convenience we label the various dihydrogen sites as *r*, *s* = C, B, A, where C corresponds to free dihydrogen, B to an intermediate, and A to the final

(20) Binsch, G. *J. Am. Chem. Soc.* **1969**, *91*, 1304.

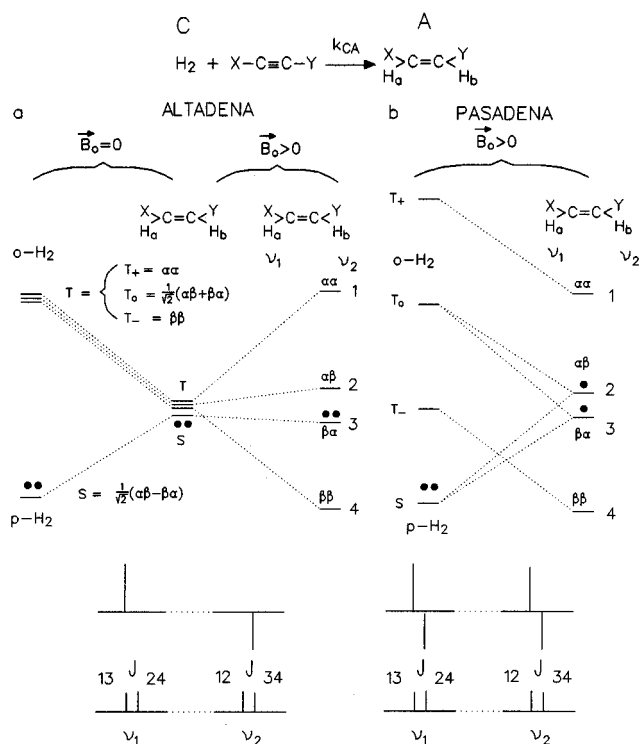


Figure 2. Scheme of (a) an ideal ALTADENA and (b) a PASADENA experiment involving the direct production of the final state A from the enriched free precursor p-H₂ (site C) with the rate constant k_{CA} . In the ALTADENA experiment the reaction is carried out outside the magnetic field B_0 , and then the sample is transferred adiabatically into the magnetic field of the NMR spectrometer for recording the NMR spectrum. In the PASADENA experiment the whole experiment is carried out in a constant magnetic field. The resulting signal patterns are compared below to the normal patterns.

hydrogenation product. These site labels should not be confused with the capital letters which are commonly used to classify nuclear two-spin systems:²¹ if a site r is characterized by the coupling constant J^r and the chemical shift difference of the two protons $\Delta\nu^r = |\nu_1^r - \nu_2^r|$, the corresponding spin system is referred to as an "AX spin system" if $J^r/\Delta\nu^r \ll 1$, as an "AB spin system" if $J^r/\Delta\nu^r \approx 1$, and as an "A₂ spin system" if $J^r/\Delta\nu^r \gg 1$.

If all p-H₂ molecules are suddenly added at the same time to a double or triple bond of an organic precursor, i.e., they are transferred from site C to site A, the signal pattern of the incorporated protons in A exhibit very strong components in adsorption and emission as indicated schematically in Figure 2 for the simple AX case, whereby $J^A/\Delta\nu^A \ll 1$. The individual signal components are about 4 orders of magnitude stronger than usually obtained for a thermal Boltzmann polarization. This high polarization results in a signal/noise gain on the order of 10^6 – 10^8 , and can also be transferred to heteronuclei of interest. Therefore, pure p-H₂ and, with some restrictions, also o-H₂ provide interesting tools for the study of hydrogenation reactions, in particular for the investigation of catalytic reactions.^{4,6,7}

The actual polarization pattern depends strongly on the details of when and where the symmetry is broken. In the ALTADENA experiment (Figure 2a) the reaction $C \rightarrow A$ is performed outside of the magnetic field whereby the two former p-H₂ protons in A remain in the singlet state. After the end of the reaction the nuclear spin symmetry in A is slowly broken by an adiabatic transfer of the sample into the magnetic field of

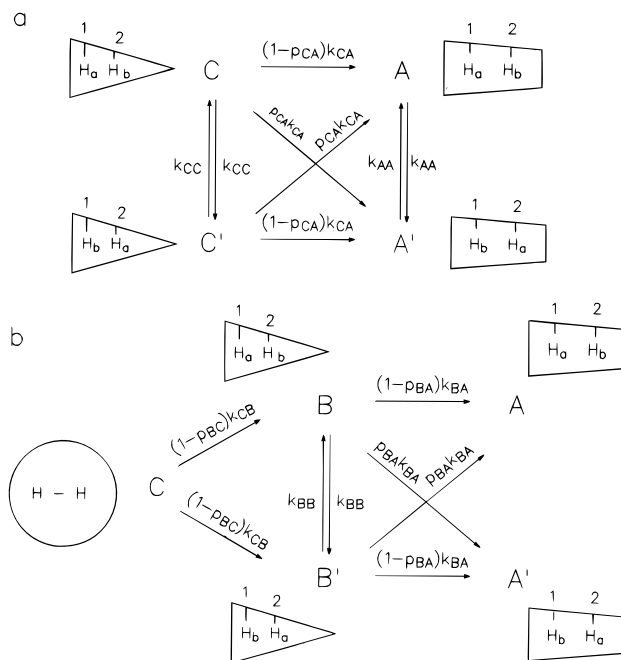


Figure 3. Formal two-site (a) and three-site (b) reaction models of the hydrogenation reaction of Figure 1. $p_{rs} = p_{sr}$, $r, s = A-C$, represents the parameter characterizing the probability of permutation of the two hydrogen atoms during the interconversion between r and s . The step is called regiospecific if $p_{rs} = 0$ or 1, nonregiospecific if $p_{rs} = 0.5$, and regioselective otherwise.

the NMR spectrometer. As a result, only the lower spin state $|3\rangle = |\beta\alpha\rangle$ becomes populated. Accordingly, after application of a $(\pi/4)_x$ pulse only two lines are observed, one in absorption and one in emission as indicated in Figure 2c. This pattern visualizes the population difference of the two states $|2\rangle = |\alpha\beta\rangle$ and $|3\rangle = |\beta\alpha\rangle$. In the PASADENA experiment (Figure 2b), however, the reaction is performed within the strong magnetic field of the NMR spectrometer itself, and thus the nuclear spin symmetry is assumed to be broken by a sudden change from C to A. As a result, the two spin eigenstates $|\alpha\beta\rangle$ and $|\beta\alpha\rangle$ in site A are created with equal probabilities and at the same time a quantum coherence is created between these states, which evolves periodically with a frequency given by the energy difference between the two states (not illustrated in Figure 2). This coherence does not affect the spectra in the AX case, however. The resulting situation is symbolized in Figure 2d, from which it follows that two pairs of lines with equal intensity are observed, whereby each pair consists of one line in absorption and one line in emission.

Exchange Model for the Time Dependence of the Nuclear Spin Density Matrix. Since the synchronous sudden reaction of all p-H₂ is not probable, we consider in this study two reaction models depicted in Figure 3. In Figure 3a only two sites, $r = C$ and A , are included. For simplicity, only the forward reactions are shown, but in the formalism also the backward reactions are included. The definition of the rate constants is straightforward. As in our previous study¹⁵ of the incoherent dihydrogen exchange, we include in both sites C and A the possibility for incoherent exchange, of the two hydrogen atoms H_a and H_b, characterized by the rate constants k_{CC} and k_{AA} . In addition, we introduce a parameter p_{CA} characterizing the regioselectivity of the reaction between C and A. p_{CA} represents the probability of permutation of the two hydrogen atoms during the transfer from C to A and A to C, respectively. The step is regiospecific if $p_{CA} = 0$ or 1, nonselective if it leads to hydrogen scrambling when $p_{CA} = 0.5$, and regioselective for other values of p_{CA} . It will be shown later that this regioselectivity requires

(21) Emsley, J. W.; Feeney, J.; Sutcliffe, L. H. *High Resolution NMR Spectroscopy*; Pergamon Press: Oxford, 1965; Vol. 1.

that the two protons are labeled prior to the reaction by different Larmor frequencies; otherwise it does not affect the results as is the case if C corresponds to free dihydrogen. However, the regioselectivity is important when an additional intermediate B is included in the more general case of Figure 3b in which the two former p-H₂ protons are chemically different.

Since we are focusing our interests to liquid samples, we consider only the high-resolution spin Hamiltonian H in which all anisotropic interactions of the spin system are neglected. Then we set up the corresponding Liouville superoperator in Liouville space and the equation of motion of the density matrix ρ . Its diagonal elements describe the populations of the spin states and its off-diagonal elements the coherences. These procedures are straightforward and have been described previously in detail by Binsch²⁰ and Ernst et al.²² Whereas Binsch was only interested in the zero and single quantum coherences needed for describing NMR line shapes, the treatment of Ernst et al. refers to the total density matrix. In order to describe general PHIP effects, a description of all density matrix elements is needed. Therefore, we will use in the following the formalism and the notation of Ernst et al.²²

Let S and I denote the two spins considered and r the index which describes the different exchanging sites. For simplicity only two sites r and s are considered for the moment. The two-spin Hamiltonian of site r is then given as usual by

$$\hat{H}^r = \nu_1^r \hat{I}_{z1}^r + \nu_2^r \hat{I}_{z2}^r + J \hat{I}_1^r \hat{I}_2^r \quad (1)$$

From these site Hamiltonians the site Liouville superoperators L^r were constructed following the procedure of Ernst et al.²²

$$L^r = \hat{H}^r \otimes \hat{E}^s - \hat{E}^r \otimes \hat{H}^s \quad (2)$$

The Liouville superoperator L of the exchange problem is given as the direct sum of the site superoperators, i.e.

$$L = L^r \oplus L^s \quad (3)$$

According to Binsch²⁰ the various kinetic processes in Figure 3 can be described by an exchange superoperator X . Its elements are derived in a straightforward way using the methods of formal chemical kinetics, treating each population and coherence like a chemical species. In practice, the elements of X are either zero or given by the products of the pseudo-first-order rate constants k_{rs} times the probability of the process. Examples of both self-exchange processes within the same or between different sites have been described in the literature.²³

Here, the intramolecular dihydrogen exchange in site r is given by X^{rr} , constructed by the corresponding permutation of the two protons in the Liouville subspace of r and the exchange between different sites r and s by X^{rs} , which connects the two Liouville subspaces. The exchange superoperator X is given as

$$X = X^{rr} \oplus X^{ss} + X^{rs} \quad (4)$$

Relaxation effects were treated on a phenomenological Bloch basis, assuming diagonal relaxation superoperators R . For each site a single T_1 relaxation rate for the populations and a single T_2 relaxation rate for the coherences were considered, i.e.

$$R = R^r \oplus R^s \quad (5)$$

The state of the system can be described by the density matrix

$$\rho = \rho^r \oplus \rho^s \quad (6)$$

Since we are interested in p-H₂-induced polarizations, which

are 4 orders of magnitude stronger than the thermal equilibrium polarization, for simplicity the limit of infinite temperature for the equilibrium density matrix can be assumed, i.e., $\rho_\infty = 0$. The time evolution of the system is then determined by the following von Neumann equation:

$$(d/dt)\rho = -(R + X + iL)\rho = -W\rho \quad (7)$$

The formal solution of this equation is

$$\rho(t) = \exp(-Wt) \rho(0) \quad (8)$$

The three-site exchange problem is a straightforward extension of the above equations; i.e., the Liouville space consists now of three site subspaces (r , s , t) with their corresponding site Liouville superoperators L^r , L^s , and L^t , site relaxation operators R^r , R^s , and R^t , intrasite self-exchange operators X^{rr} , X^{ss} , and X^{tt} , and intermolecular exchange operators X^{rs} , X^{rt} , and X^{st} given by

$$L = L^r \oplus L^s \oplus L^t \quad (9)$$

$$R = R^r \oplus R^s \oplus R^t \quad (10)$$

$$X = X^{rr} \oplus X^{ss} \oplus X^{tt} + X^{rs} + X^{rt} + X^{st} \quad (11)$$

$$\rho = \rho^r \oplus \rho^s \oplus \rho^t \quad (12)$$

We chose the four product spin Zeeman functions $|1\rangle = |\alpha\alpha\rangle$, $|2\rangle = |\alpha\beta\rangle$, $|3\rangle = |\beta\alpha\rangle$, and $|4\rangle = |\beta\beta\rangle$ of the two-spin system as base functions for the matrix representation of the site Hamiltonians in their Hilbert spaces. From these the 16 Liouville space base functions of a site Liouville space and the $16N$ base functions of the whole composite Liouville space were constructed (Table 1).

In the actual calculations we started with the initial condition that at the start of the reaction all molecules are in the p-H₂ state of site C, i.e., a pure singlet spin state. The density matrix of the p-H₂ substate is then given by

$$\begin{aligned} \rho(0) &= |S_0\rangle \\ &= |S_0\rangle\langle S_0| \\ &= (1/2)|\alpha\beta - \beta\alpha\rangle\langle\alpha\beta - \beta\alpha| \\ &= (1/4)(|E\rangle) - (1/2)(|2S_x'\rangle + |2S_y'\rangle + |2S_z'\rangle) \quad (13) \end{aligned}$$

All intermolecular exchange reactions were treated as one-sided reactions; i.e., the rates of the back reactions were set to zero.

Details of the Numerical Calculations. The density matrix of the system and the superoperator W were expressed in the base of the Liouville space described above. The matrix exponentials in the course of the time evolution of the density operator were calculated using a Padé²⁴ approximation. We assumed a reaction time of $t_r = 10$ s, which is a typical experimental value for hydrogenations. Backward rate constants from A to B and to C were set to zero. The spectra resulting from a $(\pi/4)_x$ read-out pulse were calculated by diagonalizing

(22) Ernst, R. R.; Bodenhausen, G.; Wokaun, A. *Principles of NMR in One and Two Dimensions*; Clarendon Press: Oxford, 1987.

(23) Limbach, H. H. *Dynamic NMR Spectroscopy in the Presence of Kinetic Hydrogen Deuterium Isotope Effects. NMR Basic Principles and Progress*; Berlin, Heidelberg, New York, 1991; Chapter 2.

(24) (a) Moler, C. B.; Van Loan, C. F. *Siam Rev.* **1978**, *20*, 801. (b) Golub, G. H.; Van Loan, C. F. *Matrix Computation*; John Hopkins University Press: Baltimore, 1983, Chapter 11.

Table 1. Base Functions of the Liouville Subspace for a Given Site *r*

$ \alpha\alpha\alpha\rangle = \alpha\alpha\rangle\langle\alpha\alpha $	$ \alpha\alpha\beta\rangle = \alpha\alpha\rangle\langle\alpha\beta $	$ \alpha\alpha\beta\alpha\rangle = \alpha\alpha\rangle\langle\beta\alpha $	$ \alpha\alpha\beta\beta\rangle = \alpha\alpha\rangle\langle\beta\beta $
$ \alpha\beta\alpha\rangle = \alpha\beta\rangle\langle\alpha\alpha $	$ \alpha\beta\beta\rangle = \alpha\beta\rangle\langle\alpha\beta $	$ \alpha\beta\beta\alpha\rangle = \alpha\beta\rangle\langle\beta\alpha $	$ \alpha\beta\beta\beta\rangle = \alpha\beta\rangle\langle\beta\beta $
$ \beta\alpha\alpha\rangle = \beta\alpha\rangle\langle\alpha\alpha $	$ \beta\alpha\beta\rangle = \beta\alpha\rangle\langle\alpha\beta $	$ \beta\alpha\beta\alpha\rangle = \beta\alpha\rangle\langle\beta\alpha $	$ \beta\alpha\beta\beta\rangle = \beta\alpha\rangle\langle\beta\beta $
$ \beta\beta\alpha\rangle = \beta\beta\rangle\langle\alpha\alpha $	$ \beta\beta\beta\rangle = \beta\beta\rangle\langle\alpha\beta $	$ \beta\beta\beta\alpha\rangle = \beta\beta\rangle\langle\beta\alpha $	$ \beta\beta\beta\beta\rangle = \beta\beta\rangle\langle\beta\beta $

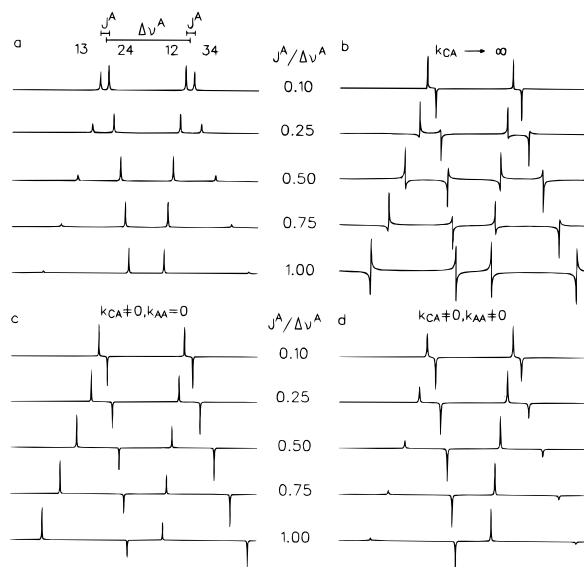


Figure 4. (a) Calculated normal NMR spectrum of a two-proton spin system of a compound A as a function of the ratio $J^A/\Delta\nu^A$. (b) Calculated PHIP patterns of the two protons in a hydrogenation product A, produced in a PASADENA experiment with $(\pi/4)_x$ pulses by the two-site reaction $C \rightarrow A$. The parameter $J^A/\Delta\nu^A$ is varied, and it is assumed that $k_{CA} \rightarrow \infty$. All signals show dispersive components. (c) Same as (b), but a reaction time $t_r = 10$ s and a rate constant $k_{AA} = 1$ s $^{-1}$ were employed, leading to pure absorption and emission lines. The ratio of the absolute outer and inner line intensities differ from those of the normal spectra. (d) Same as (c), but a self-exchange of the two protons during the reaction time t_r was introduced with $k_{AA} = 1$ s $^{-1}$, resulting in relative absolute PHIP signal intensities corresponding to those of the normal NMR spectra.

W using routine ZGEEV from the LAPACK program package²⁵ and transforming the detection operator and the density operator into the eigenbase of W.

Adiabatic changes were modeled by small stepwise changes from the initial superoperator W_i to the final W_f . We used the independence of the final density operator on the number of steps as a criterion for the adiabaticity of the change. For most calculations, between 64 and 512 steps were sufficient. Throughout all simulations a chemical shift difference of $\Delta\nu^A = 69$ Hz was assumed. All other parameters were varied.

Results and Discussion

Calculations of PASADENA Patterns for the Case of a Two-Site Reaction. For the two-site reaction $C \rightarrow A$ depicted in Figure 3a performed under PASADENA conditions, we calculated the resulting PHIP pattern of the site A as a function of the ratio $J^A/\Delta\nu^A$. The results of these calculations are depicted in Figure 4 whereby each set of spectra had its own normalization constant. In Figure 4a are shown as a reference the normal calculated NMR signals obtained for a Boltzmann equilibrium of the density matrix. In Figure 4b are depicted the PHIP spectra obtained after an instantaneous population of the site A corresponding to $k_{CA} \rightarrow \infty$. In the AX case where $J^A/\Delta\nu^A \ll 1$ the well-known pattern indicated in Figure 2b

results as discussed above. However, in the AB case strong phase distortions arise because of the imaginary parts of the zero quantum coherences ρ_{23} and ρ_{32} created between the states $|2\rangle = |\alpha\beta\rangle$ and $|3\rangle = |\beta\alpha\rangle$. These phase distortions are strongly reduced if a finite reaction rate is chosen, i.e., $k_{CA} \ll J^A, \Delta\nu^A$ (Figure 4c), leading to a successive population of site A. As a result, ρ_{23} and ρ_{32} become real and the signals obtained by the $(\pi/4)_x$ pulse appear in either pure enhanced absorption or emission. The absolute intensities of the outer lines are larger than those of the inner lines, in contrast to the pattern of the normal spectra of Figure 4a.

Next we investigated the effect of an incoherent mutual exchange of the two protons in the product site A according to Figure 3a, characterized by the rate constant k_{AA} . The latter was set equal to a value substantially smaller than J^A , but large enough to accomplish full magnetization transfer during the reaction time $t_r = 10$ s. This leads to a complete disappearance of the zero quantum coherences. As illustrated in Figure 4d, now the absolute line intensities of the inner lines are larger than those of the outer lines, as in the case of the normal spectra. These magnetization transfer effects are most pronounced in the case of the AB case where $J^A/\Delta\nu^A \approx 1$ (bottom spectrum). By contrast, AX-type spectra are practically not influenced by the exchange, neglecting the minor broadening effect of the lines by the exchange which is not important for the present discussion.

Calculations of the PASADENA pattern for regioselectivities p_{CA} between 0 and 1 showed that the resulting density matrices and, therefore, the calculated PHIP spectra are independent of this parameter. This is the expected result because in p-H₂ the two protons are indistinguishable.

In conclusion, if the spin system in site A exhibits an AX character, the well-known PASADENA signal pattern results; however, when the spin system is of the AB type, the resulting PHIP signal pattern is different, depending on the kinetics of the hydrogenation and of the dihydrogen exchange in the products. This agrees with experimental findings, which have been previously⁷ interpreted in terms of a singlet/triplet mixing between the $|S_0\rangle$ and the $|T_0\rangle$ states which are not eigenstates. Thus, if $J^A/\Delta\nu^A \approx 1$, the PASADENA experiment could be used as a very sensitive probe for measuring slow self-exchange rates in the product A, although these rates may also be obtained by other NMR methods.

Calculations of ALTADENA \rightarrow PASADENA Changes for a Two-Site Reaction. In recent ALTADENA experiments PASADENA-like polarization patterns have been observed.²⁶ Since it appeared that such effects could again result from magnetization transfer in site A during the adiabatic field cycling process, we simulated the outcome of ALTADENA experiments in terms of the two-site reaction model of Figure 3a as a function of k_{AA} . The results of these simulations are depicted in Figure 5, and they show that indeed a transition from the ALTADENA-type signal pattern to the PASADENA-type pattern occurs if k_{AA} is increased even at values $k_{AA} \ll \Delta\nu^A$. Therefore, in terms of the two-site reaction network of Figure 3a, the observation of PASADENA-type signal patterns in an ALTADENA experiment would provide evidence for a slow magnetization transfer

(25) LAPACK Program package, University of California, Berkeley, 1994, distributed by AT&T Laboratories New Jersey. E-mail address: netlib@research.att.com.

(26) Haake, M.; Barkemeyer, J.; Bargon, J. *J. Phys. Chem.* **1995**, 99, 17539. Haake, M.; Barkemeyer, J.; Bargon, J. Unpublished results.

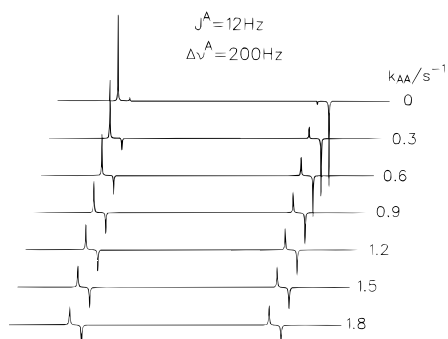


Figure 5. Calculated PHIP patterns of the two protons in the hydrogenation product A produced by the two-site reaction $C \rightarrow A$ in an ALTADENA experiment as a function of the rate constant k_{AA} of incoherent dihydrogen exchange in the product A under the condition $J^A/\Delta\nu^A \ll 1$. Thereby it is assumed that the magnetic field is switched on adiabatically after the reaction time $t_r = 10$ s before applying a $(\pi/4)_x$ reading pulse. The PHIP pattern evolves from the typical ALTADENA to the PASADENA pattern as k_{AA} is increased.

in the product site A, in a similar way as the transformation of the signal pattern of Figure 4c to the pattern of Figure 4d in a PASADENA-type experiment.

Calculations of PASADENA Signal Patterns for the Case of a Three-Site Reaction. We felt that the results of the previous section were not yet entirely satisfactory for the following reasons: in a typical hydrogenation product A the two former p-H₂ atoms are bound to carbon, where the barrier to the exchange of the two particles is very large. On the other hand, free dihydrogen cannot be the cause of magnetization transfer effects in the PHIP spectra of A, because this would require two different Larmor frequencies for both protons. Therefore, we studied the question of whether these effects could instead arise from an intermediate B exhibiting one of the chemical structures illustrated in Figure 1, where dihydrogen is mobile, according to the three-site-reaction network of Figure 3b described theoretically in the previous section. In other words, our aim was to look for evidence of the intermediate B derived from the PHIP pattern of the product A, even though B cannot directly be observed.

In the line shape simulations we proceeded in a similar way as in the case of the two-site-reaction model, but always set $k_{AA} = 0$ and assumed that the condition $J^A/\Delta\nu^A \approx 1$ is satisfied. The results showed that under certain conditions one can really observe effects of B upon the PHIP pattern of A.

The first condition is that the chemical shifts and coupling constants in site B and A are different, because otherwise both sites cannot be distinguished by NMR and the evolution of the spin density matrix is the same in both environments.

If B constitutes an A₂ spin system, i.e., if $J^B/\Delta\nu^B \gg 1$ holds, the singlet state of the p-H₂ is an eigenstate of both sites C and B, and the nuclear symmetry is not broken until the last step B \rightarrow A. In this case the PHIP pattern of A is not dependent on the properties of B, and the three-site model reduces to the two-site model. However, this case can be excluded if the PHIP pattern of A shows signs of magnetization transfer as indicated in Figures 4d and 5.

By contrast, if B constitutes an AX- or AB-type spin system, the PHIP pattern of A carries information on B. In this case, the breaking of the nuclear symmetry already occurs in the first step C \rightarrow B and the evolution of the spin system, while it is in the B state, can be different from the evolution in site A. The effect of this intermediate obviously depends on the values of the rate constants k_{CB} and k_{BA} as compared to the parameters k_{BB} , J^B , and $\Delta\nu^B$. Especially the value of k_{BA} is of great

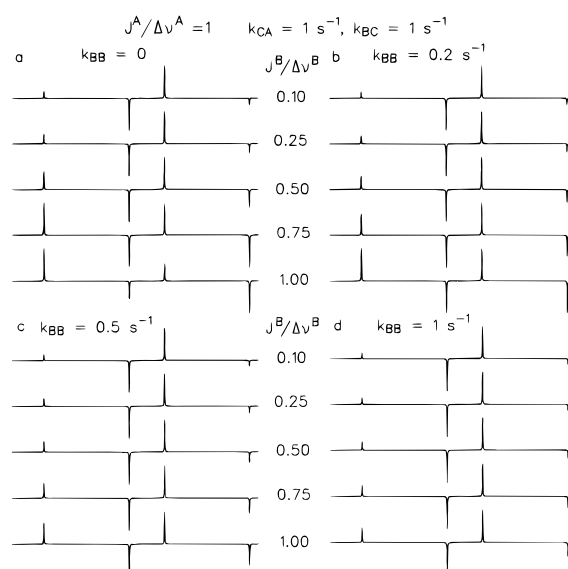


Figure 6. Calculated PHIP signal patterns of a hydrogenation product A resulting in a PASADENA experiment in the presence of the three-site reaction $C \rightarrow B \rightarrow A$ as a function of the ratio $J^B/\Delta\nu^B$ and the self-exchange rate k_{BB} of the intermediate B. For further explanation see the text.

importance. If it is much larger than k_{BB} , πJ^B , and $\pi\Delta\nu^B$, the spin system has no time to evolve during the lifetime of B, which then has no influence, and the model reduces to the two-site reaction model. The absolute values of k_{CB} mainly influence only the absolute but not the relative PHIP line intensities provided that k_{CB} does not lead to an instantaneous formation of B, which could lead again to line distortions discussed in Figure 4b.

Therefore, in the calculations we varied mainly the ratio $J^B/\Delta\nu^B$ and the rate constants k_{BB} of the incoherent dihydrogen exchange in B, as well as the regioselectivity parameter p_{BA} of the last step—as defined in Figure 3b—while using the fixed rate constant values $k_{CB} = k_{BA} = 1$ s⁻¹ for convenience.

Figure 6 shows the resulting PASADENA signal patterns of A formed in the three-site reaction of Figure 3b. The four sets of spectra illustrate the influence of k_{BB} and of $J^B/\Delta\nu^B$. If B constitutes an AX spin system because $J^B/\Delta\nu^B \ll 1$, the resulting spectra show no dependence on k_{BB} as can be seen by comparing the top spectra of Figure 6a–d. In this case the ratio between the absolute intensities of the outer and the inner lines corresponds to the normal spectrum. However, if B constitutes an AB spin system as expected in the case of substantial but not too large exchange couplings, i.e., if $J^B/\Delta\nu^B$ is increased, large effects are observed. Now, the ratio between the absolute intensities of the outer and the inner lines increases as compared to the normal spectrum (Figure 6a, bottom).

As k_{BB} is increased, this effect disappears gradually as a comparison of the bottom spectra of Figure 6 a–d shows; eventually, a situation is reached where the ratio between the absolute intensities of the inner and the outer line intensities corresponds to the normal spectra (not shown) as if a magnetization transfer in A had occurred. Thus, in principle, the incoherent dihydrogen exchange, the exchange and magnetic couplings, and the chemical shifts of the two protons in the intermediate B all leave fingerprints which can be deciphered from the PHIP pattern of A.

Another interesting finding is the influence of the regioselectivity parameter p_{BA} associated with the step B \rightarrow A. Some of our results are depicted in Figure 7. The regioselective case $p_{BA} = 0$ is identical to the case $k_{BB} = 0$ depicted in Figure 6a.

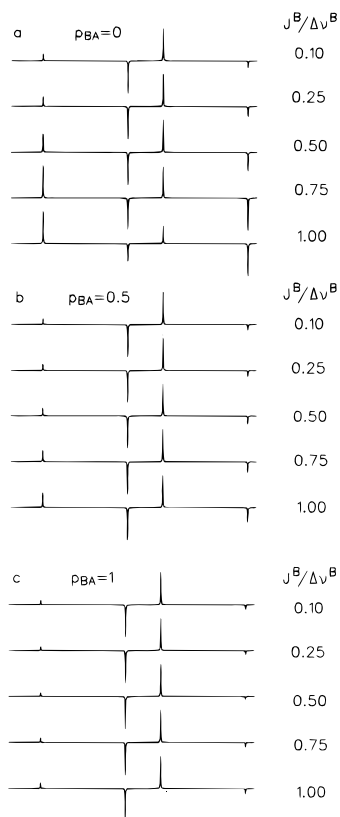


Figure 7. Calculated PHIP signal patterns of a hydrogenation product A resulting in a PASADENA experiment in the presence of the three-site reaction $C \rightarrow B \rightarrow A$ as a function of the ratio $J^B/\Delta\nu^B$ and the selectivity parameter p_{BA} . For further explanation see the text.

This case is expected if both the dihydrogen and the substrate are complexed to the metal (Figure 1, pathway iii). In the other case of a regiospecific reaction, i.e., if $p_{BA} = 1$, a somewhat different pattern results, indicating the dependence of the effects on the chemical shift changes between B and A. Essentially, this case is equivalent to that where the chemical shifts in one of the sites are reversed or where p_{BA} changes from 0 to 1. The case of a lack of any regioselectivity, i.e., $p_{BA} = 0.5$, is found to be equivalent with the case of a complete magnetization transfer depicted in Figure 6d. This condition is expected either for pathway i in Figure 1, whereby the dihydrogen becomes activated by binding to the metal and is subsequently transferred to free substrate, or alternatively for pathway ii, whereby free dihydrogen is transferred to an activated substrate-transition metal complex.

Finally, we note that in both cases, i.e., irrespective of whether there is a magnetization transfer in B with $k_{BB} \neq 0$ or a lack of

regioselectivity with $p_{BA} = 0.5$, both pathways lead to a transition from ALTADENA- to PASADENA-type signal patterns of A, as long as the reaction takes place during the adiabatic field cycling process in a way similar to that mentioned above for the two-site reaction model. The advantage of this concept is that one no longer needs to invoke magnetization transfer within the stable hydrogenation product A; instead an AX or AB spin system in the intermediate B will accomplish this task. Since the absence of magnetization transfer in A can easily be verified independently in a separate NMR experiment, the ALTADENA experiment, therefore, also constitutes an interesting tool for the characterization of an otherwise elusive intermediate of type B.

Conclusions

A dynamic model for the calculation of parahydrogen-induced nuclear polarization (PHIP) of hydrogenation products has been described which is based on the density matrix formalism as proposed by Binsch.²⁰ Using numerical simulations typical for actual experiments, it can be shown that the PHIP patterns depend not only on the type of experiment performed—e.g., ALTADENA in the absence and PASADENA in the presence of a magnetic field—but also on the properties of possible reaction intermediates where the reactants are bound to the employed transition metal catalyst. The important parameters of the intermediate are the chemical shifts and coupling constants of the former p-H₂ protons, especially their exchange couplings, as well as the rate of an incoherent dihydrogen exchange. In addition, the regioselectivity of the hydrogenation step is a factor determining the PHIP patterns, whereby the individuality of the former p-H₂ proton atoms arises from different chemical shifts in the intermediate.

The model used and the results obtained here represent a previously missing theoretical link between the phenomena of incoherent and coherent dihydrogen exchange in transition metal hydrides and the PHIP effect, a connection which has so far not yet been recognized. Moreover, PHIP is again identified as a powerful and sensitive tool to study reaction pathway effects via analysis of the polarization patterns of the final hydrogenation products.

Applications of the model as described in this paper to actual experiments are in progress. In addition, we currently extend the model to larger spin systems including deuterium.

Acknowledgment. This work was supported by the Deutsche Forschungsgemeinschaft, Bonn, the Freie Universität Berlin, the Stiftung Volkswagenwerk, Hannover, and the Fonds der Chemischen Industrie, Frankfurt.

JA954188B